# Antibacterial effect of polylactic-*co*-glycolic acid/selenium nanocomposite against dental biofilm

**Mohsen Safaei**[1), 2)] (ORCID ID: 0000-0003-3885-6640), **Farnoosh Khaleseh**[3)] (0009-0004-4610-198X), **Saba Ahmadi**[3)] (0009-0006-4100-1714), **Mohammad Salmani Mobarakeh**[2)] (0000-0002-3272-6640), **Douglas Law**[4)] (0000-0002-7824-3542), **Ling Shing Wong**[4)] (0000-0002-9571-0804), **D. Ravinder**[5)] (0000-0002-0626-3034), **Amos Nhlapo**[6), *)] (0000-0001-5670-4056), **Mohd Hashim**[7)] (0000-0003-0231-0697), **Azra Parveen**[7)] (0000-0003-2444-3503)

DOI: https://doi.org/10.14314/polimery.2025.3.4

**Abstract:** To determine the optimal conditions for obtaining poly(lactic-*co*-glycolic) acid with selenium (PLGA/selenium) nanocomposites the Taguchi method was used. FT-IR, Raman spectroscopy, XRD and FESEM analysis confirmed the nanocomposites' structure. The nanocomposite containing 6 mg/mL of selenium obtained in the process where the mixing time was 75 min showed the highest antibacterial activity against *Streptococcus mutans*. The obtained nanocomposites are an innovative approach to improving oral health and can be used as antibacterial materials for medical and dental applications.

**Keywords:** poly(lactic-*co*-glycolic acid), selenium, nanocomposite, *Streptococcus mutans*, human health, Taguchi method.

## Działanie antybakteryjne nanokompozytu poli(kwasu mlekowego-*co*-glikolowego) z selenem na biofilm zębowy

**Streszczenie:** Metodą Taguchi określono optymalne warunki otrzymywania nanokompozytów poli(kwasu mlekowego-*co*-glikolowego) z selenem (PLGA/selen) i oceniono ich aktywność przeciwbakteryjną przeciwko *Streptococcus mutans*. Najwyższą aktywnością przeciwbakteryjną charakteryzował się nanokompozyt zawierający 6 mg/mL selenu (czas mieszania 75 min). Strukturę nanokompozytu potwierdzono metodą FT-IR, spektroskopii Ramana, XRD i FESEM. Nanokompozyty PLGA/selen stanowią nowe podejście do poprawy zdrowia jamy ustnej i mogą być stosowane jako materiały przeciwbakteryjne do zastosowań medycznych i stomatologicznych.

**Słowa kluczowe:** kwas poli(mlekowy-*co*-glikolowy), selen, nanokompozyt, *Streptococcus mutans*, ludzkie zdrowie, metoda Taguchi.

The indiscriminate and inappropriate use of antibiotics in medical and dental treatments has led to the emergence of antibiotic-resistant bacteria, posing a significant global health concern [1]. Dental caries, classified as a chronic oral disease, can compromise overall health and, despite extensive efforts, continues to be highly prevalent [2]. *Streptococcus mutans*, a bacterium that plays a pivotal role in the development of dental caries, is capable of producing extracellular polymers within dental biofilms [3]. The growing problem of microbial antibiotic resistance, which is linked to human health, necessitates novel approaches. Nanotechnology offers a promising strategy to combat resistant bacteria [4]. Nanotechnology involves the study of particles at the nanoscale. It finds applications in various fields, including medicine. The goal of nanomedicine is to develop products and materials that improve health and personal care [5].

Poly(lactic-*co*-glycolic acid), owing to its favourable structural properties, has numerous applications in nanomedicine. This polymer is a copolymer of alpha-

[1)] Division of Dental Biomaterials, School of Dentistry, Kermanshah University of Medical Sciences, Kermanshah 54658, Iran.
[2)] Advanced Dental Sciences and Technology Research Center, School of Dentistry, Kermanshah University of Medical Sciences, Kermanshah 38647, Iran.
[3)] Students Research Committee, Kermanshah University of Medical Sciences, Kermanshah, Iran.
[4)] Faculty of Health and Life Sciences, INTI International University, Nilai 71800, Malaysia.
[5)] Department of Physics, Osmania University, Telangana, 500007, Hyderabad, India.
[6)] Department of Medical Physics, Sefako Makgatho Health Sciences University, P. O. Box 146, Medunsa 0204, South Africa.
[7)] Department of Applied Physics, Aligarh Muslim University, Aligarh, India.
[*)] Author for correspondence: amos.nhlapo@smu.ac.za

-hydroxy propanoic acid (polylactic acid) and hydroxy acetic acid (glycolic acid) [6]. PLGA exhibits properties such as biodegradability, biocompatibility, and hydrophobicity, contributing to its widespread use. The degradation rate of PLGA can be controlled by the ratio of lactic acid to glycolic acid. By regulating the degradation of this polymer, the release and distribution of the desired substance or drug can be controlled [6, 7].

Selenium is widely used in various fields, including physics, chemistry, and biology. A significant property of selenium is its antimicrobial activity, attributed to its ability to catalyse the oxidation of thiols within cells, leading to the death of microorganisms and demonstrating its bactericidal properties [8]. Selenium possesses both therapeutic and preventive properties. Its biocompatibility, low toxicity, and novel therapeutic properties have garnered attention, leading to its incorporation into nanocomposites [9]. Nanotechnology employs methods to maintain particle size within the nanoscale, enabling their use for various purposes. Historically, nanotechnology was primarily applied in physics and chemistry, but over time, biological scientists have recognized its benefits in diverse fields. Nanodentistry, a branch of nanotechnology, utilizes nanotechnology for the prevention, diagnosis, and treatment of oral diseases [10]. Additionally, nanotechnology can be applied to dental drugs, opening new horizons in the field of dentistry [11].

In this study, the Taguchi method was employed to synthesize the nanocomposite under optimal conditions. This cost-effective method enables the attainment of high-quality results without increasing costs [12]. The nanocomposite used in this study comprises selenium reinforcement within a PLGA polymer matrix. The objective of this study is to introduce the PLGA-selenium nanocomposite and investigate its antibacterial effects against *S. mutans*.

## EXPERIMENTAL PART

### Materials

PLGA used in this study was purchased from Merck. Selenium nanoparticles were obtained according to the following process. *Halomonas elongata* (IBRC-M 10433) bacteria, which were sourced from the Iranian Biological Resource Center, were utilized to create selenium nanoparticles. The bacterial growth medium was made by mixing 0.75 g of glucose, 3 g of NaCl, 0.028 g of $K_2HPO_4$, and 0.0001 g of $FeSO_4$ in 100 mL of distilled water and then agitating the mixture with a magnetic stirrer. Following sterilization in an autoclave, a colony of bacteria was transferred to Erlenmeyer flasks. The bacteria and growth medium in the Erlenmeyer flasks were then incubated at 37°C for 48 hours. The bacteria were subsequently isolated from the growth medium through centrifugation at 5000 rpm for 5 min, and the resulting supernatant was retained for nanoparticle production. The supernatant was combined with solutions containing 0.8 mg/mL of sodium selenite in a 1:1 ratio. The resultant solutions were placed in a shaking incubator at 30°C and 140 rpm for 48 h. The produced nanoparticles were isolated and purified via centrifugation at 5000 rpm for 15 min. The resulting solutions were autoclaved at 80°C for 24 h to prepare the nanoparticle powder for structural analysis [13, 14].

#### Synthesis of PLGA/selenium nanocomposites

To investigate and determine the optimal conditions for producing nanocomposites with the strongest antibacterial properties, the experiments were formulated using the Qulitek-4 software based on the Taguchi method [15]. To determine the optimal synthesis conditions of the nanocomposite using the direct mixing method, different concentrations of PLGA polymer (2, 4, and 6 mg/mL) were used along with different concentrations of selenium nanoparticles (4, 6, and 8 mg/mL), as well as different stirring times (45, 60, and 75 min). Solutions containing the polymer and nanoparticles were each stirred separately using a magnetic stirrer for one hour. An ultrasonic homogenizer was then used to disperse the two solutions for 15 min at room temperature. Finally, the selenium nanoparticle solution was added dropwise to the PLGA polymer solution. The resulting solution was stirred for one hour and then dispersed for 15 min. To synthesize the final nanocomposite, the previously prepared solution was placed in an oven at 60°C for 24 h, resulting in the formation of nanocomposite precipitates. The resulting precipitate was extracted using a spatula and then ground in a mortar to produce the final nanocomposite powder [15, 16].

### Methods

#### Antibacterial activity

To investigate the antimicrobial effect of the synthesized PLGA/selenium nanocomposite on *Streptococcus mutans* biofilms, the bacterium (ATCC 35668) was obtained from Iranian Industrial Microorganisms Collection Center. To obtain a single colony, the bacteria were cultured on agar for 24 h. Then, a bacterial suspension corresponding to 0.5 McFarland was carefully prepared. To initiate the formation of bacterial biofilm, the bacterial suspension was placed in a 96-well plate and incubated at 37°C for 72 h. After the formation, the biofilm was washed three times with phosphate buffer solution (PBS) to remove any remaining planktonic cells. Then, the synthesized nanocomposites, carefully prepared by the Taguchi method, were added to each well. Then, the plate was incubated for 24 h. To determine the number of viable cells in the biofilm, cells extracted from the well wall were collected after a 24 h incubation period at 37°C. After three washes, the remaining cells that adhered to the well wall were

suspended in 1 ml of phosphate-buffered saline. The resulting suspension was mixed by a vortex for 2 min. To perform the colony-forming unit (CFU) assay, the bacterial suspensions were subjected to 10-fold serial dilution before plating on agar plates. The plates were then placed in an incubator at 37°C for 24 h, and the number of colonies was counted. Finally, the average number of colonies was determined for 9 experiments, each with three replicates [17, 18].

**FT-IR spectroscopy**

Fourier Transform Infrared (FT-IR) spectroscopy was employed to examine the structural and chemical characteristics of the synthesized nanomaterials. The FT-IR spectra of the synthesized nanocomposite and its components were recorded using a Fourier Transform Infrared Spectrometer (Avatar 360, Thermo Nicolet, Waltham, MA, USA) in the range of 400-4000 $cm^{-1}$ under ambient temperature conditions after preparing sample pellets.

**Raman spectroscopy**

Raman spectroscopic analysis was performed using a Teksan (Tehran, Iran) spectrometer with a 532 nm laser.

**X-ray diffraction**

The analysis of X-ray diffraction (XRD) was performed using a Philips PW1730 diffractometer (Amsterdam, Netherland) (40 kV, 30 mA) to determine the size, identify the phase, and assess the crystalline structure. The sample was irradiated with X-rays at various angles 2θ between 20 and 80 degrees, and the XRD pattern was obtained by measuring the diffraction rate. This allowed the assessment of the scattering intensity curve as a function of the angle 2θ, using X-rays with a wavelength $\lambda$ (K$\alpha$-Cu $\lambda$=1.54 Å). This curve exhibited peaks at specific angles corresponding to the distance between crystal planes, facilitating the determination of the crystalline structure of the samples.

**T a b l e 1. Composition and synthesis conditions of the nanocomposites determined by the Taguchi method**

| Sample | PLGA mg/mL | Stirring time min | Selenium NPs mg/mL |
|---|---|---|---|
| 1 | 2 | 45 | 4 |
| 2 | 2 | 60 | 6 |
| 3 | 2 | 75 | 8 |
| 4 | 4 | 45 | 6 |
| 5 | 4 | 60 | 8 |
| 6 | 4 | 75 | 4 |
| 7 | 6 | 45 | 8 |
| 8 | 6 | 60 | 4 |
| 9 | 6 | 75 | 6 |

**Field Emission Scanning Elector Microscopy**

A Tescan MIRA3 (Kohoutovice, Czech Republic) field emission scanning electron microscope (FESEM) operating at 30 kV was used to obtain images of the synthesized nanocomposite. Subsequently, an analysis of the nanocomposite's absorption spectrum was performed. For this purpose, after sample preparation, the spectrum of the constituent elements was collected using an EDX detector with a Bruker instrument on a field emission scanning electron microscope (Quantax, Bruker, Billerica, MA, USA). Additionally, elemental mapping was performed on the surface to investigate the distribution of elements in the nanocomposite.

## RESULTS AND DISCUSSION

**Antibacterial activity**

To determine the optimal conditions for obtaining PLGA/selenium nanocomposites with the most effective antibacterial properties, nine experiments were conducted using the Taguchi method (Table 1). The effects of the synthesized nanocomposites under different conditions on bacterial survival were evaluated and recorded in Fig. 1. The results showed that the nanocomposite synthesized under experimental condition 9, with 6 mg/mL PLGA, 75 min of stirring time, and 6 mg/mL selenium nanoparticles, exhibited the strongest antibacterial activity against *S. mutans* biofilm. In the presence of this nanocomposite, the lowest bacterial survival rate was observed at Log10 CFU/mL 18/0. Figure 2 shows the effects of PLGA, stirring time, and selenium nanoparticles on the survival of *Streptococcus mutans*. The results indicate that the aforementioned factors at level 3 had the greatest impact on reducing the survival of this bacterium.

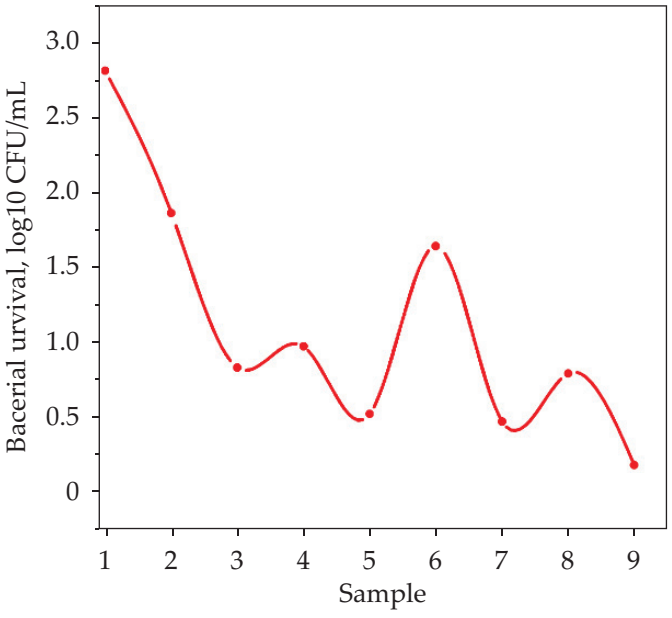


**Fig. 1. Antibacterial activity of PLGA/selenium nanocomposites**

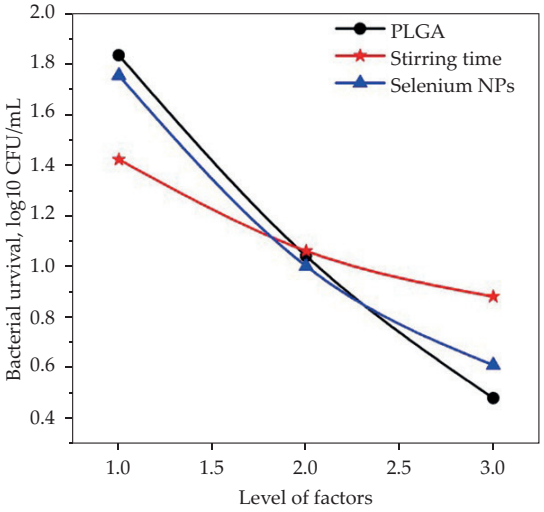


**Fig. 2. Effects of different levels of PLGA, stirring time and selenium NPs on the survival of *Streptococcus mutans* biofilm**

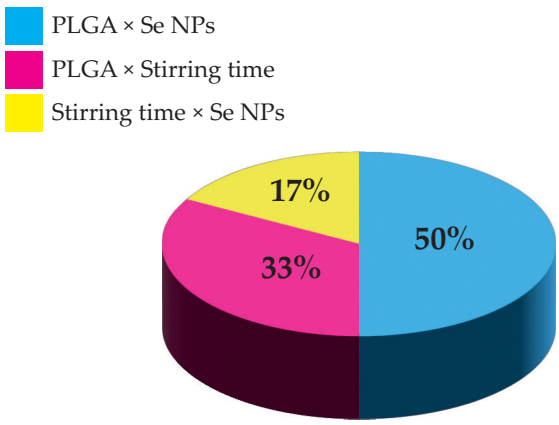


**Fig. 3. Interactions effects of studied factors on the survival of *Streptococcus mutans* biofilm**

**T a b l e 2. Analysis of variance of factors influencing the limitation of Streptococcus mutans biofilm growth**

| Factors | DOF | Sum of squares | Variance | F-Ratio F | Pure Sum | Percent % |
|---|---|---|---|---|---|---|
| PLGA | 2 | 2.77 | 1.39 | 8.42 | 2.44 | 43.99 |
| Stirring time | 2 | 0.44 | 0.22 | 1.35 | 0.11 | 2.07 |
| Selenium | 2 | 2.01 | 1.00 | 6.10 | 1.68 | 30.25 |

DOF - degree of freedom.

In this study, the interaction effects of numerous factors on the growth of *S. mutans* were also investigated, as shown in Figure 3. Specifically, stirring time at level 3 and selenium nanoparticles at level 2 had the highest interaction effect (32.6%). Additionally, level 3 of PLGA and stirring time showed a significant interaction effect on bacterial survival (50.9%). In contrast, the interaction effect index for PLGA at level 3 and selenium nanoparticles at level 2 (32.5%) was the lowest. Table 2 contains the results of the analysis of variance for the factors influencing the viability of *S. mutans*. In that order, the factors that had the greatest impact on bacterial survival were PLGA (44%), selenium nanoparticles (30.3%), and stirring time (2.1%).

After a thorough analysis of the data and an examination of the effects of each factor and their interactions, the optimal conditions for the synthesis of PLGA/selenium nanocomposites with the highest level of antibacterial activity were accurately estimated and tabulated (Table 3). The findings revealed that PLGA had the greatest impact on bacterial survival, while stirring time had the least impact. On the other hand, selenium nanoparticles showed an effect between these two factors, closer to PLGA.

It was also determined that level 3 was the most suitable level for the PLGA, stirring time, and selenium nanoparticle factors. Based on the results, it was found that the synthesized nanocomposite effectively inhibited bacterial activity under optimal conditions at –0.27 $Log_{10}$ CFU/mL (completely inhibiting bacterial growth), which was better than the results of all nine experiments conducted.

**T a b l e 3. Optimum conditions for the synthesis of PLGA/selenium nanocomposite with the highest antibacterial activity**

| Factors | Level | Contribution |
|---|---|---|
| PLGA | 3 | 0.64 |
| Stirring time | 3 | 0.24 |
| Selenium | 3 | 0.51 |
| Total contribution from all factors | | 1.39 |
| Current grand average of performance | | 1.12 |
| Bacterial survival at optimum condition | | -0.27 |

## FT-IR analysis

FT-IR spectra of the PLGA biopolymer, selenium nanoparticles, and PLGA/selenium nanocomposite, in the wavelength range of 400–4000 $cm^{-1}$ are shown in Fig. 4. The regions at 3023 and 2949 $cm^{-1}$ in the FT-IR spectrum of PLGA indicate the stretching vibrations of aliphatic C-H. Additionally, the absorption of the carbonyl group (C=O) of PLGA is observed at 1762 $cm^{-1}$. The stretching vibrations in the range of 1389 to 1452 $cm^{-1}$ confirm the presence of the $CH_2$ group next to the carbonyl group [19]. Using the FT-IR, we have shown different functional

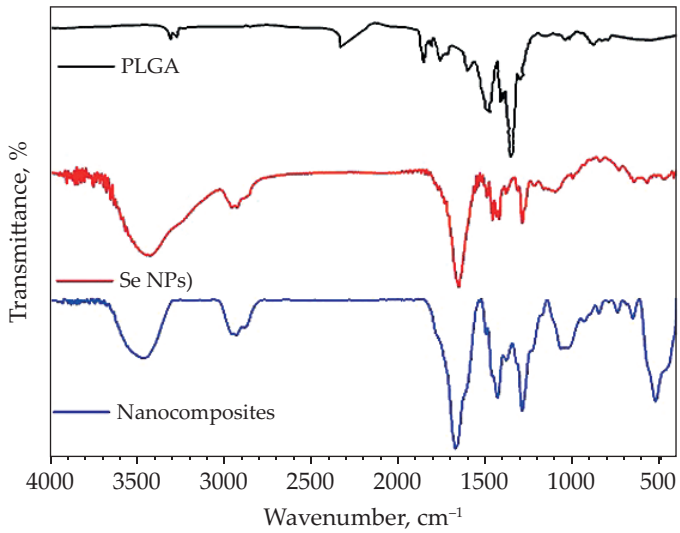


**Fig. 4. FT-IR spectra of PLGA, selenium NPs, PLGA/selenium nanocomposite**

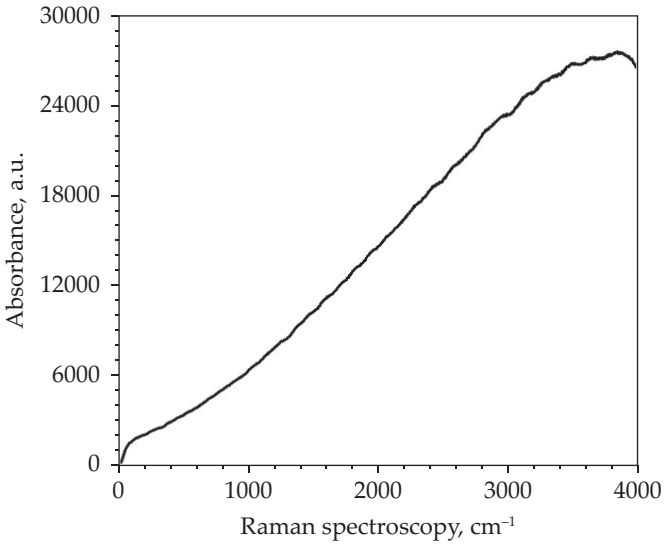


**Fig. 5. Raman spectroscopy of PLGA/selenium nanocomposite**

groups involved in the reduction of selenium nanoparticles. Two main peaks in the FT-IR spectrum of selenium nanoparticles, located at 3423 $cm^{-1}$ and 1653 $cm^{-1}$ respectively, indicate the stretching of hydroxyl groups. Also, the peak observed at 1290 $cm^{-1}$ corresponds to C=O, –NH, and -$NH_2$ functional groups. These functional groups, in addition to providing stability to selenium nanoparticles, are also known as reducing agents and convert sodium selenite to elemental selenium [13].

The various peaks observed in the FT-IR spectrum of the final nanocomposite indicate the presence of both the polymeric matrix and selenium nanoparticles. These peaks also indicate the interaction and dependence between the components of the nanocomposite [20].

## Raman spectroscopy

The geometry of molecules, the evaluation of their structure, and the determination of chemical bonds and molecular structure of the synthesized PLGA/selenium nanocomposite were performed by obtaining its Raman spectroscopy pattern using a 532 nm wavelength. In Figure 5, the peaks corresponding to PLGA are observed at 850, 1050, 1450, and 1750 $cm^{-1}$, and the peaks corresponding to selenium are observed at 250 and 450 $cm^{-1}$.

## XRD analysis

The X-ray diffraction patterns are presented in Figure 6. The semi-crystalline structure of PLGA was confirmed by the presence of a broad peak in the X-ray diffraction pattern of this copolymer at a 2θ angle of 21 degrees [19]. The selenium nanoparticles were formed with good crystallinity, which is indicated by the narrow and sharp peaks in their X-ray diffraction pattern. These peaks are located at 2θ values of 23.5, 29.2, 41.4, 43.3, 45.4, 52.5, 55.7, and 62.7, corresponding to the crystal planes (100), (101), (110), (102), (111), (201), (112), and (202), respectively, which is in accordance with the standard card (JCPDS card No. 06-362) [13]. A comparison of the X-ray diffraction pattern of the synthesized nanocomposite with its components shows that the peak positions have shifted to the right or left. Also, some peaks in the X-ray diffraction pattern of the nanocomposite components have decreased or increased in intensity or have disappeared. These results confirm the interaction of the constituent components of the nanocomposite and its formation.

## SEM and EDS analysis

In Figure 7a), the appearance and morphology of the PLGA-selenium nanocomposite, prepared using a field emission scanning electron microscope at a magnifica-

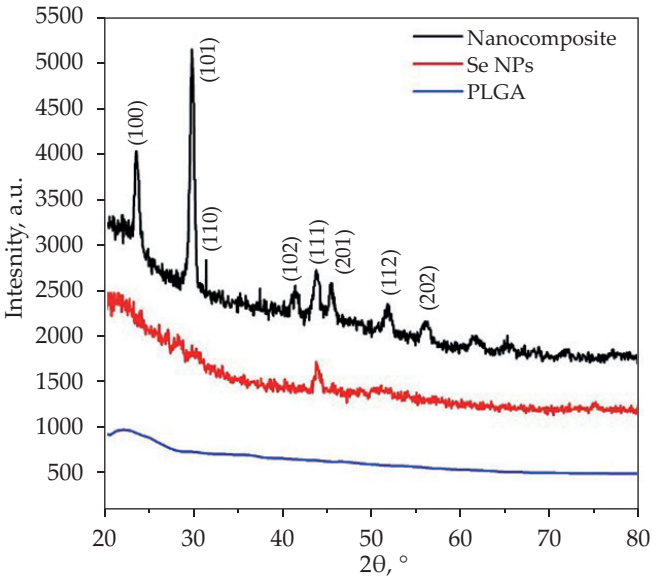


**Fig. 6. XRD patterns of PLGA, selenium NPs and PLGA/selenium nanocomposite**

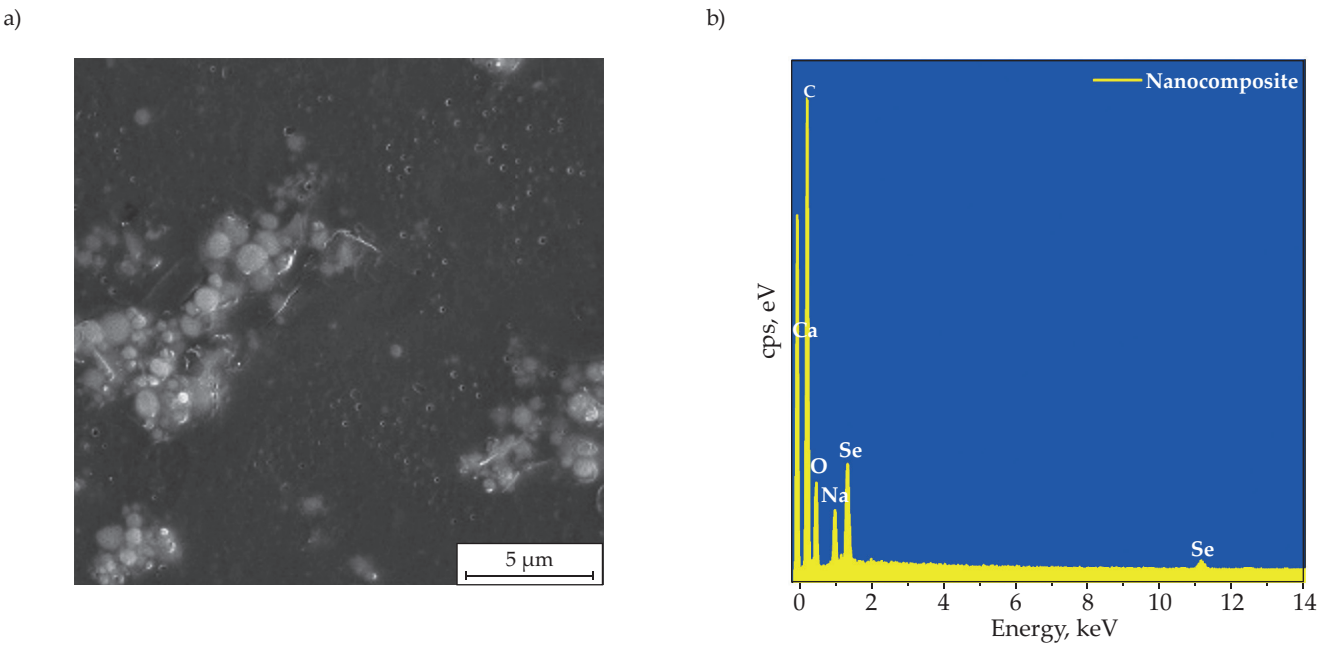


**Fig. 7. Results of SEM and EDX analyses of PLGA/selenium nanocomposite: a) SEM image, b) EDX pattern**

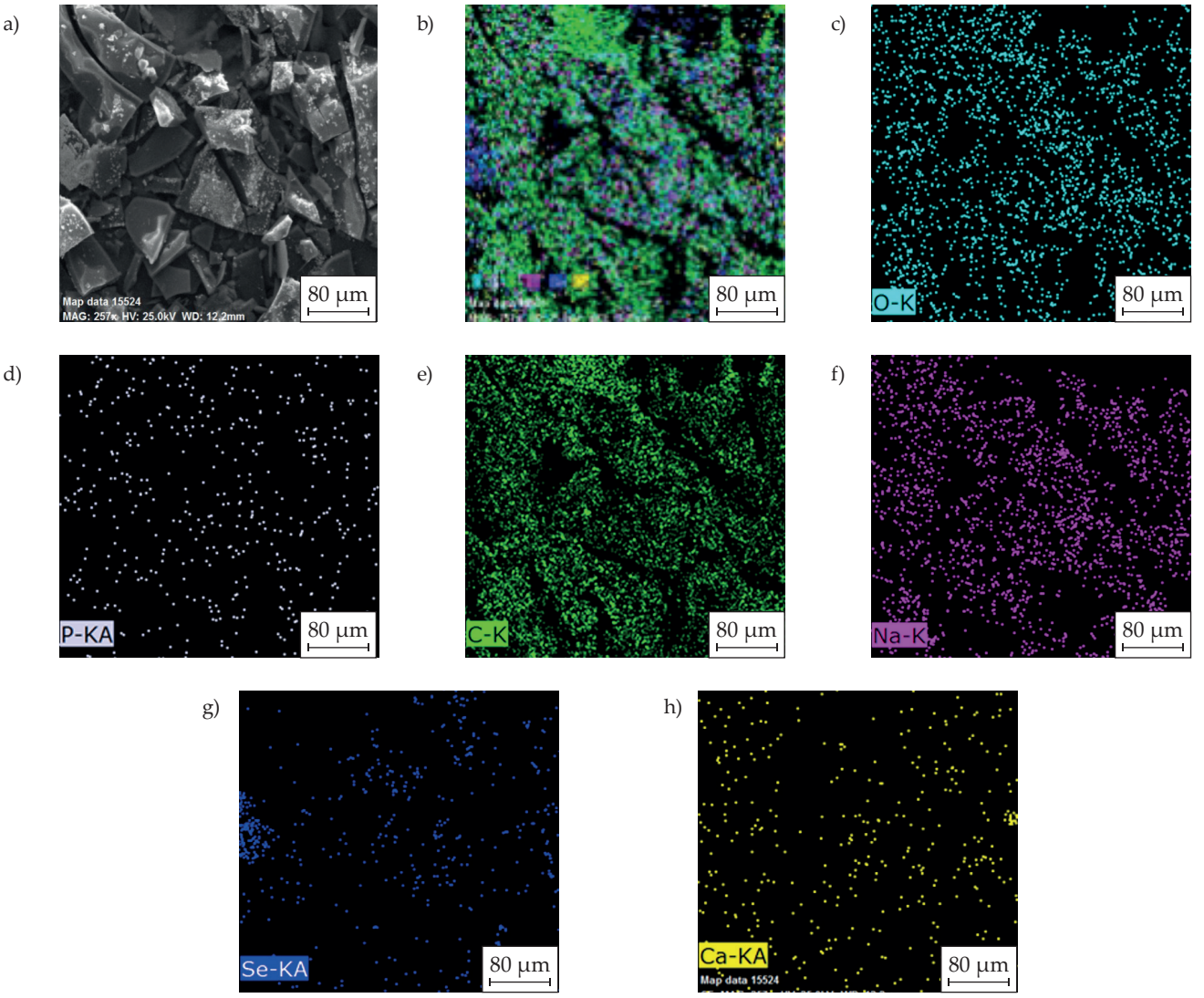


**Fig. 8. Dispersion map of the nanocomposite composition: a) surface image, b) all elements, c) oxygen, d) phosphorus, e) carbon, f) sodium, g) selenium, h) calcium**

tion of 5 microns, were investigated. In this image, selenium nanoparticles can be seen as dark spots in the light polymer matrix. The size of the selenium nanoparticles varied and was in the range of 50 to 100 nanometers. The elements present in the PLGA-selenium nanocomposite were identified using energy dispersive X-ray spectroscopy (EDS) analysis. The obtained spectrum is depicted in Figure 7b). The presence of carbon (85.6 wt%), oxygen (25.74 wt%), selenium (3.77 wt%), sodium (2.61 wt%), and calcium (0.03 wt%) as the constituent elements of the nanocomposite confirmed its formation

**Element mapping analysis**

Figure 8 shows a map of the distribution of these elements in the outer layer of the nanocomposite. Also, the uniform distribution of elements in the overall structure of the produced nanocomposite indicates the formation of a nanocomposite with a uniform and desirable structure.

## CONCLUSIONS

Using the Taguchi method for experimental design, the PLGA/selenium nanocomposite synthesized by direct mixing was analyzed and evaluated for its antibacterial activity against the S. *mutans* bacterial strain, and its desirable antibacterial properties were confirmed. This nanocomposite, considering its predicted antibacterial properties, can make a positive change in the fight against bacterial biofilms. The synthesized nanocomposite was found to completely inhibit the growth of bacteria under optimal conditions based on the results of antibacterial activity tests. Moreover, the synthesized nanocomposite showed desirable structural properties using various characterization methods. Therefore, this composite has the potential to significantly reduce pathogenic pathogens and treatment costs and prevent dental diseases.

*ACKNOWLEDGEMENTS*
*The authors gratefully acknowledge the Students Research Committee of Kermanshah University of Medical Sciences (grant number: 990439) for financial support.*

***Authors contribution***
M.S. - investigation, methodology, visualization; F.K. - conceptualization, investigation; S.A. - investigation; M.S.M. - writing-original draft, writing-review and editing; D.L. - resources, writing-review and editing; L.S.W. - resources, writing-review and editing; D.R. - data analysis, supervision; A.N. - conceptualization, methodology, project administration; M.H. - validation, writing-original draft; A.P. - validation, writing-original draft.

***Funding***
The research was funded by the Kermanshah University of Medical Sciences under Grant No 990439.

***Conflict of interest***
The authors declare no conflict of interest.



REFERENCES

[1] Cella E., Giovanetti M., Benedetti F. *et al.*: *Pathogens* **2023**, *12*, 1074. https://doi.org/10.3390/pathogens12091074
[2] Cheng L, Zhang L., Yue L. *et al.*: *International Journal of Oral Science* **2022**, *14*, 17. https://doi.org/10.1038/s41368-022-00167-3
[3] Huang X., Zhang K., Deng M. *et al.*: *Archives of Oral Biology* **2017**, *82*, 256. https://doi.org/10.1016/j.archoralbio.2017.06.026
[4] Brar B., Marwaha S., Poonia A.K. *et al.*: *Archives of Microbiology* **2023**, *205*, 62. https://doi.org/10.1007/s00203-023-03404-3
[5] Satalkar P., Elger B.S., Shaw D.W.: *Science and Engineering Ethics* **2016**, *22*, 1255. https://doi.org/10.1007/s11948-015-9705-6
[6] Rocha C.V., Gonçalves V., da Silva M.C. *et al.*: *International Journal of Molecular Sciences* **2022**, *23*, 2034. https://doi.org/10.3390/ijms23042034
[7] Hua Y., Su Y., Zhang H. *et al.*: *Drug Delivery* **2021**, *28*, 1342. https://doi.org/10.1080/10717544.2021.1943056
[8] Shoeibi S., Mozdziak P., Golkar-Narenji A.: *Topics in Current Chemistry* **2017**, *375*, 88. https://doi.org/10.1007/s41061-017-0176-x
[9] Tsivileva O., Pozdnyakov A., Ivanova A.: *Molecules* **2021**, *26*, 3657. https://doi.org/10.3390/molecules26123657
[10] Sreenivasalu P.K.P., Dora C.P., Swami R. *et al.*: *Nanomaterials* **2022**, *12*, 1676. https://doi.org/10.3390/nano12101676
[11] Sundaram G., Ramakrishnan T., H. Parthasarathy H. *et al.*: *Journal of Indian Society of Periodontology* **2018**, *22*, 122. https://doi.org/10.4103/jisp.jisp_322_17
[12] Mohrazi A., Ghasemi-Fasaei R., Mojiri A. *et al.*: *Polymers* **2023**, *15*, 3778. https://doi.org/10.3390/polym15183778
[13] Safaei M., Mozaffari H.R., Moradpoor H. *et al.*: *Advances in Materials Science and Engineering* **2022**, *2022*, 1376998. https://doi.org/10.1155/2022/1376998

[14] Moradpoor H., Safaei M., Golshah A. *et al*.: *Inorganic Chemistry Communications* **2021**, *130*, 108748. https://doi.org/10.1016/j.inoche.2021.108748
[15] Safaei M., Taran M.: *Journal of Polymers and the Environment* **2022**, *30*, 2066. https://doi.org/10.1007/s10924-021-02329-6
[16] Safaei M., Moghadam A.: *Materials Today Communications* **2022**, *31*, 103698. https://doi.org/10.1016/j.mtcomm.2022.103698
[17] Zhang G., Lu M., Liu R. *et al*.: *Frontiers in Microbiology* **2020**, *11*, 774. https://doi.org/10.3389/fmicb.2020.00774
[18] Chamlagain M, Hu J., Sionov R.V. *et al*.: *Frontiers in Microbiology* **2024**, *15*, 1333274. https://doi.org/10.3389/fmicb.2024.1333274
[19] Bahari Javan N., Rezaie Shirmard L., Jafary Omid N. *et al*.: *Journal of Microencapsulation* **2016**, *33*, 460. https://doi.org/10.1080/02652048.2016.1208296
[20] Husseina A.A., Mutar M.A., Ficai A.: *Journal of Ceramic Processing Research* **2024**, *25*, 178. https://doi.org/10.36410/jcpr.2024.25.2.178

*Received 20 XII 2024.*
*Accepted 17 II 2025.*